ISA Transactions ■ (■■■■) ■■■–■■■

Contents lists available at ScienceDirect

ISA Transactions

journal homepage: www.elsevier.com/locate/isatrans

Research Article

Position and attitude tracking control for a quadrotor UAV

Jing-Jing Xiong *, En-Hui Zheng

College of Mechanical and Electrical Engineering, China Jiliang University, Hangzhou 310018, PR China

ARTICLE INFO

Article history:
Received 3 November 2013
Received in revised form
29 December 2013
Accepted 16 January 2014
This paper was recommended for publication by Jeff Pieper.

Keywords:
Quadrotor UAV
Underactuated
Novel robust TSMC
SMC
Synthesis control

ABSTRACT

A synthesis control method is proposed to perform the position and attitude tracking control of the dynamical model of a small quadrotor unmanned aerial vehicle (UAV), where the dynamical model is underactuated, highly-coupled and nonlinear. Firstly, the dynamical model is divided into a fully actuated subsystem and an underactuated subsystem. Secondly, a controller of the fully actuated subsystem is designed through a novel robust terminal sliding mode control (TSMC) algorithm, which is utilized to guarantee all state variables converge to their desired values in short time, the convergence time is so small that the state variables are acted as time invariants in the underactuated subsystem, and, a controller of the underactuated subsystem is designed via sliding mode control (SMC), in addition, the stabilities of the subsystems are demonstrated by Lyapunov theory, respectively. Lastly, in order to demonstrate the robustness of the proposed control method, the aerodynamic forces and moments and air drag taken as external disturbances are taken into account, the obtained simulation results show that the synthesis control method has good performance in terms of position and attitude tracking when faced with external disturbances.

1. Introduction

The quadrotor unmanned aerial vehicles (UAVs) are being used in several typical missions, such as search and rescue missions, surveillance, inspection, mapping, aerial cinematography and law enforcement [1–5].

Considering that the dynamical model of the quadrotor is an underactuated, highly-coupled and nonlinear system, many control strategies have been developed for a class of similar systems. Among them, sliding mode control, which has drawn researchers' much attention, has been a useful and efficient control algorithm for handling systems with large uncertainties, time varying properties, nonlinearities, and bounded external disturbances [6]. The approach is based on defining exponentially stable sliding surfaces as a function of tracking errors and using Lyapunov theory to guarantee all state trajectories reach these surfaces in finite-time, and, since these surfaces are asymptotically stable, the state trajectories slides along these surfaces till they reach the origin [7]. But, in order to obtain fast tracking error convergence, the desired poles must be chosen far from the origin on the left half of *s*-plane, simultaneously, this will, in turn, increase the gain of the controller, which is undesirable considering the actuator saturation in practical systems [8,9].

Replacing the conventional linear sliding surface with the nonlinear terminal sliding surface, the faster tracking error convergence is to obtain through terminal sliding mode control (TSMC). Terminal sliding mode has been shown to be effective for providing faster convergence than the linear hyperplane-based sliding mode around the equilibrium point [8,10,11]. TSMC was proposed for uncertain dynamic systems with pure-feedback form in [12]. In [13], a robust adaptive TSMC technique was developed for *n*-link rigid robotic manipulators with uncertain dynamics. A global non-singular TSMC for rigid manipulators was presented in [14]. Finite-time control of the robot system was studied through both state feedback and dynamic output feedback control in [15]. A continuous finite-time control scheme for rigid robotic manipulators using a new form of terminal sliding modes was proposed in [16]. For the sake of achieving finite-time tracking control for the rotor position in the axial direction of a nonlinear thrust active magnetic bearing system, the robust non-singular TSMC was given in [17]. However, the conventional TSMC methods are not the best in the convergence time, the primary reason is that the convergence speed of the nonlinear sliding mode is slower than the linear sliding mode when the state variables are close to the equilibrium points. In [18], a novel TSMC scheme was developed using a function augmented sliding hyperplane for the guarantee that the tracking error converges to zero in finite-time, and was proposed for the uncertain single-input and single-output (SISO) nonlinear system with unknown external disturbance. In the most of existing research results, the uncertain external disturbances are not taken into account these nonlinear systems. In order to further demonstrate the robustness of novel

* Corresponding author.
E-mail addresses: jjxiong357@gmail.com (J.-J. Xiong), ehzheng@cjlu.edu.cn (E.-H. Zheng).

0019-0578/$ - see front matter © 2014 ISA. Published by Elsevier Ltd. All rights reserved.
http://dx.doi.org/10.1016/j.isatra.2014.01.004

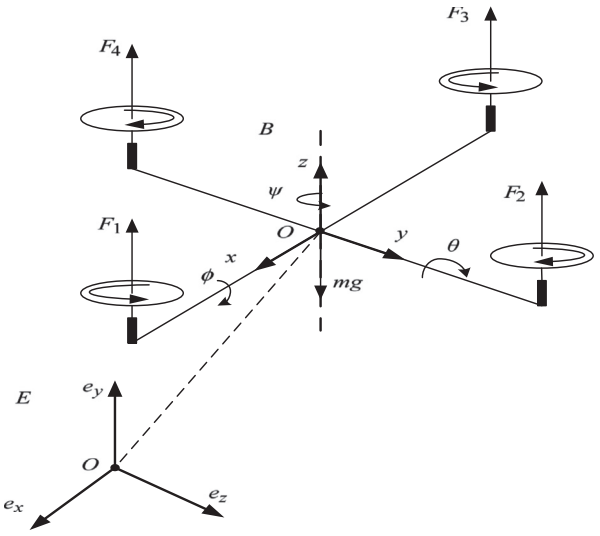

Fig. 1. Quadrotor UAV.

TSMC, the external disturbances are considered into the nonlinear systems and are applied to the controller design.

In this work, we combine two components in the proposed control: a novel robust TSMC component for high accuracy tracking performance in the fully actuated subsystem, and a SMC component that handles the external disturbances in the under-actuated subsystem.

Even though many classical, higher order and extended SMC strategies, have been developed for the flight controller design for the quadrotor UAV (see for instance [19–23], and the list is not exhaustive), and, these strategies in the papers [19–23] were utilized to dictate a necessity to compensate for the external disturbances, in addition, the other control methods, such as proportional–integral–differential (PID) control [24,25], backstepping control [26,27], switching model predictive attitude control [28], etc., have been proposed for the flight controller design, most of the aforementioned control strategies have been proposed in order to make the quadrotor stable in finite-time and the stabilization time of the aircraft may be too long to reflect the performance of them. In addition, the stabilization time is essential significance for the quadrotor UAV to quickly recover from some unexpected disturbances. For the sake of decreasing the time, a synthesis control method based on the novel robust TSMC and SMC algorithms is applied to the dynamical model of the quadrotor UAV. The synthesis control method is proposed to guarantee all system state variables converge to their desired values in short time. Furthermore, the convergence time of the state variables are predicted via the equations derived by the novel robust TSMC, this is demonstrated by the following sections.

The organization of this work is arranged as follows. Section 2 presents the dynamical model of a small quadrotor UAV. The synthesis control method is detailedly introduced in Section 3. In Section 4, simulation results are performed to highlight the overall validity and the effectiveness of the designed controllers. In Section 5, a discussion, which is based on different synthesis control schemes, is presented to emphasize the performance of the proposed synthesis control method in this work, followed by the concluding remarks in Section 6.

2. Quadrotor model

In order to describe the motion situations of the quadrotor model clearly, the position coordinate is to choose. The model of the quadrotor is set up in this work by the body-frame B and the earth-frame E as presented in Fig. 1. Let the vector $[x,y,z]'$ denotes the position of the center of the gravity of the quadrotor and the vector $[u, v,w]'$ denotes its linear velocity in the earth-frame. The vector $[p,q,r]'$ represents the quadrotor's angular velocity in the body-frame. m denotes the total mass. g represents the acceleration of gravity. l denotes the distance from the center of each rotor to the center of gravity.

The orientation of the quadrotor is given by the rotation matrix $R{:}E\rightarrow B$, where R depends on the three Euler angles $[\phi,\theta,\psi]'$, which represent the roll, the pitch and the yaw, respectively. And $\phi\in(-\pi/2,\pi/2)$, $\theta\in(-\pi/2,\pi/2)$, $\psi\in(-\pi,\pi)$.

The transformation matrix from $[\phi,\theta,\psi]'$ to $[p,q,r]'$ is given by

$$\begin{bmatrix} p \\ q \\ r \end{bmatrix} = \begin{bmatrix} 1 & 0 & -\sin\theta \\ 0 & \cos\phi & \sin\phi\cos\theta \\ 0 & -\sin\phi & \cos\phi\cos\theta \end{bmatrix} \begin{bmatrix} \dot{\phi} \\ \dot{\theta} \\ \dot{\psi} \end{bmatrix} \tag{1}$$

The dynamical model of the quadrotor can be described by the following equations [5,24,29]:

$$\begin{cases} \ddot{x} = \frac{1}{m}(\cos\phi\sin\theta\cos\psi + \sin\phi\sin\psi)u_1 - \frac{K_1\dot{x}}{m} \\ \ddot{y} = \frac{1}{m}(\cos\phi\sin\theta\sin\psi - \sin\phi\cos\psi)u_1 - \frac{K_2\dot{y}}{m} \\ \ddot{z} = \frac{1}{m}(\cos\phi\cos\theta)u_1 - g - \frac{K_3\dot{z}}{m} \\ \ddot{\phi} = \dot{\theta}\dot{\psi}\frac{I_y - I_z}{I_x} + \frac{J_r}{I_x}\dot{\theta}\Omega_r + \frac{l}{I_x}u_2 - \frac{K_4 l}{I_x}\dot{\phi} \\ \ddot{\theta} = \dot{\psi}\dot{\phi}\frac{I_z - I_x}{I_y} - \frac{J_r}{I_y}\dot{\phi}\Omega_r + \frac{l}{I_y}u_3 - \frac{K_5 l}{I_y}\dot{\theta} \\ \ddot{\psi} = \dot{\phi}\dot{\theta}\frac{I_x - I_y}{I_z} + \frac{1}{I_z}u_4 - \frac{K_6}{I_z}\dot{\psi} \end{cases} \tag{2}$$

where K_i denote the drag coefficients and positive constants; $\Omega_r = \Omega_1 - \Omega_2 + \Omega_3 - \Omega_4, \Omega_i$, stand for the angular speed of the propeller i I_x,I_y,I_z represent the inertias of the quadrotor;J_r denotes the inertia of the propeller;u_1 denotes the total thrust on the body in the z-axis;u_2 and u_3 represent the roll and pitch inputs, respectively;u_4 denotes a yawing moment.$u_1 = (F_1+F_2+F_3+F_4)$, $u_2 = (-F_2+F_4)$, $u_3 = (-F_1+F_3)$, $u_4 = d(-F_1+F_2+F_3+F_4)/b$,, where $F_i = b\Omega_i^2$ denote the thrust generated by four rotors and are considered as the real control inputs to the dynamical system, b denotes the lift coefficient;d denotes the force to moment scaling factor.

3. Synthesis control

Compared with the brushless motor, the propeller is very light, we ignore the moment of inertia caused by the propeller. Eq. (2) is divided into two parts:

$$\begin{bmatrix} \ddot{z} \\ \ddot{\psi} \end{bmatrix} = \begin{bmatrix} \frac{u_1\cos\phi\cos\theta}{m} - g \\ \frac{1}{I_z}u_4 \end{bmatrix} + \begin{bmatrix} -\frac{K_3}{m}\dot{z} \\ \dot{\phi}\dot{\theta}\frac{I_x - I_y}{I_z} - \frac{K_6}{I_z}\dot{\psi} \end{bmatrix} \tag{3}$$

$$\begin{cases} \begin{bmatrix} \ddot{x} \\ \ddot{y} \end{bmatrix} = \frac{u_1}{m}\begin{bmatrix} \cos\psi & \sin\psi \\ \sin\psi & -\cos\psi \end{bmatrix}\begin{bmatrix} \cos\phi\sin\theta \\ \sin\phi \end{bmatrix} + \begin{bmatrix} -\frac{K_1}{m}\dot{x} \\ -\frac{K_2}{m}\dot{y} \end{bmatrix} \\ \begin{bmatrix} \ddot{\phi} \\ \ddot{\theta} \end{bmatrix} = \begin{bmatrix} l/I_x & 0 \\ 0 & l/I_y \end{bmatrix}\begin{bmatrix} u_2 \\ u_3 \end{bmatrix} + \begin{bmatrix} \dot{\theta}\dot{\psi}\frac{I_y - I_z}{I_x} - \frac{K_4 l}{I_x}\dot{\phi} \\ \dot{\psi}\dot{\phi}\frac{I_z - I_x}{I_y} - \frac{K_5 l}{I_y}\dot{\theta} \end{bmatrix} \end{cases} \tag{4}$$

where Eq. (3) denotes the fully actuated subsystem (FAS), Eq. (4) denotes the underactuated subsystem (UAS). For the FAS, a novel robust TSMC is used to guarantee its state variables converge to their desired values in short time, then the state variables are regarded as time invariants, therefore, the UAS gets simplified. For the UAS, a sliding mode control approach is utilized. The special synthesis control scheme is introduced in the following sections.

Please cite this article as: Xiong J-J, Zheng E-H. Position and attitude tracking control for a quadrotor UAV. ISA Transactions (2014), http://dx.doi.org/10.1016/j.isatra.2014.01.004

3.1. A novel robust TSMC for FAS

Considering the symmetry of a rigid-body quadrotor, therefore, we get $I_x=I_y$ Let $x_1=[z\psi]'$and $x_2==[\dot{z}\dot{\psi}]'$. The fully actuated subsystem is written by

$$\begin{cases}\dot{x}_1=x_2,\\ \dot{x}_2=f_1+g_1u_1+d_1\end{cases} \tag{5}$$

where $f_1=[-g\ 0]', g_1=[\ \cos\phi\ \cos\theta/m\ 0;0\ \ 1/I_z\ \ ], u_1=[u_1\ \ u_4]'$ and $d_1=[-K_3\dot{z}/m-K_6\dot{\psi}/I_z]'$.

To develop the tracking control, the sliding manifolds are defined as [18,30]

$$s_2=\dot{s}_1+\omega_1 s_1+\xi_1 s_1^{m_1'/n_1'} \tag{6a}$$

$$s_4=\dot{s}_3+\omega_2 s_3+\xi_2 s_3^{m_2'/n_2'} \tag{6b}$$

where $s_1=z_d-z,\ \ s_3=\psi_d-\psi$, Z_d and ψ_d are the desired values of state variables Z and ψ, respectively. In addition, the coefficients $(\omega_1,\omega_2,\xi_1,\xi_2)$ are positive, m_1', m_2', n_1', n_2' are positive odd integers with $m_1'<n_1'$ and $m_2'<n_2'$.

Let $s_2=0$ and $s_4=0$. The convergence time is calculated as follows:

$$t_{s_1}=\frac{n_1'}{\omega_1(n_1'-m_1')}\ln\left(\frac{\omega_1[s_1(0)]^{(n_1'-m_1')/n_1'}+\xi_1}{\xi_1}\right) \tag{7a}$$

$$t_{s_3}=\frac{n_2'}{\omega_2(n_2'-m_2')}\ln\left(\frac{\omega_2[s_3(0)]^{(n_2'-m_2')/n_2'}+\xi_2}{\xi_2}\right) \tag{7b}$$

In accordance with Eq. (5) and the time derivative of s_2 and s_4, we have

$$\dot{s}_2=\ddot{z}_d-\frac{u_1}{m}\cos\phi\cos\theta+g+\frac{K_3}{m}\dot{z}+\omega_1\dot{s}_1+\xi_1\frac{d}{dt}s_1^{m_1'/n_1'} \tag{8a}$$

$$\dot{s}_4=\ddot{\psi}_d-\frac{1}{I_z}u_4+\frac{K_6}{I_z}\dot{\psi}+\omega_2\dot{s}_3+\xi_2\frac{d}{dt}s_3^{m_2'/n_2'} \tag{8b}$$

The controllers are designed by

$$u_1=\frac{m}{\cos\phi\cos\theta}\left[\ddot{z}_d+g+\omega_1\dot{s}_1+\xi_1\frac{m_1'}{n_1'}s_1^{(m_1'-n_1')/n_1'}\dot{s}_1+\varepsilon_1 s_2+\eta_1 s_2^{m_1/n_1}\right] \tag{9a}$$

$$u_4=I_z\left(\ddot{\psi}_d+\omega_2\dot{s}_3+\xi_2\frac{m_2'}{n_2'}s_3^{(m_2'-n_2')/n_2'}\dot{s}_3+\varepsilon_2 s_4+\eta_2 s_4^{m_2/n_2}\right) \tag{9b}$$

where ε_1,ε_2,η_1, and η_2 are positive,m_1, n_1, m_2, and n_2 are positive odd integers with $m_1<n_1$ and $m_2<n_2$.

Under the controllers, the state trajectories reach the areas (Δ_1,Δ_2) of the sliding surfaces $s_2=0$ and $s_4=0$ along $\dot{s}_2=-\varepsilon_1 s_2-\eta_1' s_2^{m_1/n_1}$ and $\dot{s}_4=-\varepsilon_2 s_4-\eta_2' s_4^{m_2/n_2}$ in finite-time, respectively. The time is defined as

$$t_1'\le\frac{n_1}{\varepsilon_1(n_1-m_1)}\ln\frac{\varepsilon_1[s_1(0)]^{(n_1-m_1)/n_1}+\delta_1}{\delta_1} \tag{10a}$$

$$t_2'\le\frac{n_2}{\varepsilon_2(n_2-m_2)}\ln\frac{\varepsilon_2[s_3(0)]^{(n_2-m_2)/n_2}+\delta_2}{\delta_2} \tag{10b}$$

where

$$\eta_1'=\eta_1+(-K_3\dot{z}/m)/|s_2^{m_1/n_1}|, \eta_1=L_1/|s_2^{m_1/n_1}|+\delta_1,$$
$$L_1=|K_3\dot{z}/m|_{\max}, \delta_1>0, \Delta_1=\{|s_2|\le(L_1/\eta_1)^{m_1/n_1}\}$$
$$\eta_2'=\eta_2+(-K_6\dot{\psi}/I_z)/|s_4^{m_2/n_2}|, \eta_2=L_2/|s_4^{m_2/n_2}|+\delta_2$$
$$L_2=|K_6\dot{\psi}/I_z|_{\max}, \delta_2>0, \Delta_2=\{|s_4|\le(L_2/\eta_2)^{m_2/n_2}\}$$

Proof 1. In order to illustrate the subsystem is stable, here, we only choose the state variable z as an example and Lyapunov theory is applied.

Considering the Lyapunov function candidate

$$V_1=s_2^2/2$$

Invoking Eqs. (8a) and (9a) the time derivative of V_1 is derived

$$\dot{V}_1=s_2\dot{s}_2=s_2(-\varepsilon_1 s_2-\eta_1 s_2^{m_1/n_1}+K_3\dot{z}/m)$$
$$=-\varepsilon_1 {s_2}^2-\eta_1' s_2^{(m_1+n_1)/n_1}$$

Considering that (m_1+n_1) is positive even integer, that's, $\dot{V}_1\le 0$. The state trajectories of the subsystem converge to the desired equilibrium points in finite-time. Therefore, the subsystem is asymptotically stable.

3.2. A SMC approach for UAS

In this section, the details about sliding mode control of a class of underactuated systems are found in [29]. Let $Q=\frac{u_1}{m}\begin{bmatrix}\cos\psi & \sin\psi\\ \sin\psi & -\cos\psi\end{bmatrix}$, and $y_1=Q^{-1}[x\ y]', y_2=Q^{-1}[\dot{x}\ \dot{y}]'$, $y_3=[\phi\ \theta]', y_4=[\dot{\phi}\ \dot{\theta}]'$. The underactuated subsystem is written in a cascaded form

$$\begin{aligned}&\dot{y}_1=y_2,\\ &\dot{y}_2=f_2+d_2,\\ &\dot{y}_3=y_4,\\ &\dot{y}_4=f_3+g_2u_2+d_3.\end{aligned} \tag{11}$$

According to Eqs. (9a) and (9b) we can select the appropriate parameters to guarantee the control law u_1 and yaw angle ψ converge to the desired/reference values in short time. That's,$\dot{u}_1=0$,ψ becomes time invariant, then $\dot{\psi}=0$, Q is time invariant matrix and non-singular because u_1 is the total thrust and nonzero to overcome the gravity. As a result

$$f_2=[\ \cos\phi\ \sin\theta\ \sin\phi]', d_2=Q^{-1}diag[K_1/m\ K_2/m]Qy_2, f_3=0, g_2$$
$$=diag[l/I_x\ l/I_y], u_2=[u_2\ u_3]', d_3=diag[-lK_4/I_x-lK_5/I_y]y_4$$

Define the tracking error equations

$$\begin{cases}e_1=y_1^{\mathrm{d}}-y_1,\\ e_2=\dot{e}_1=\dot{y}_1^{\mathrm{d}}-y_2,\\ e_3=\dot{e}_2=\ddot{y}_1^{\mathrm{d}}-f_2,\\ e_4=\dot{e}_3=\dddot{y}_1^{\mathrm{d}}-\left(\frac{\partial f_2}{\partial y_1}y_2+\frac{\partial f_2}{\partial y_2}f_2+\frac{\partial f_2}{\partial y_3}y_4\right)\end{cases} \tag{12}$$

where the vector y_1^{d} denotes the desired value vector.

The sliding manifolds are designed as

$$s=c_1e_1+c_2e_2+c_3e_3+e_4 \tag{13}$$

where the constants $c_i>0$.

By making $\dot{s}=-M\mathrm{sgn}(s)-\lambda s$, we get

$$u_2=\left[\frac{\partial f_2}{\partial y_3}g_2\right]^{-1}\begin{Bmatrix}c_1e_2+c_2e_3+c_3e_4+\dddot{y}_1^{\mathrm{d}}-\frac{\mathrm{d}}{\mathrm{dt}}\left[\frac{\partial f_2}{\partial y_1}y_2\right]\\ -\frac{\mathrm{d}}{\mathrm{dt}}\left[\frac{\partial f_2}{\partial y_2}f_2\right]-\frac{\mathrm{d}}{\mathrm{dt}}\left[\frac{\partial f_2}{\partial y_3}\right]y_4\\ -\frac{\partial f_2}{\partial y_3}(f_3+d_3)+M\mathrm{sgn}(s)+\lambda s\end{Bmatrix} \tag{14}$$

where

$$M=(c_2\bar{d}_2+c_3\beta_2\bar{d}_2)||E_1||_2+\beta_3\bar{d}_4||\xi(y)||_2+\rho,$$
$$\beta_1\ge\partial f_2/\partial y_1, \beta_2\ge\partial f_2/\partial y_2, \beta_3\ge\partial f_2/\partial y_3,$$
$$E_1=[e_1e_2e_3]', \xi(y)=[y_1y_2y_3y_4]' \text{ and } \lambda>0,$$
$$\rho>0, ||d_2||<\bar{d}_2||E_1||_2, \bar{d}_2=\max(K_1/mK_2/m)$$
$$||d_3||<\bar{d}_4||\xi(y)||_2, \bar{d}_4=\max(lK_4/I_xlK_5/I_y).$$

According to $\frac{\partial f_2}{\partial y_3}=[-\sin\phi\sin\theta\quad\cos\phi\cos\theta\cos\phi 0]$, and $0<||\partial f_2/\partial y_3||=|\cos^2\phi\cos\theta<2$, and , therefore, $\partial f_2/\partial y_3$ is invertible.

Please cite this article as: Xiong J-J, Zheng E-H. Position and attitude tracking control for a quadrotor UAV. ISA Transactions (2014), http://dx.doi.org/10.1016/j.isatra.2014.01.004

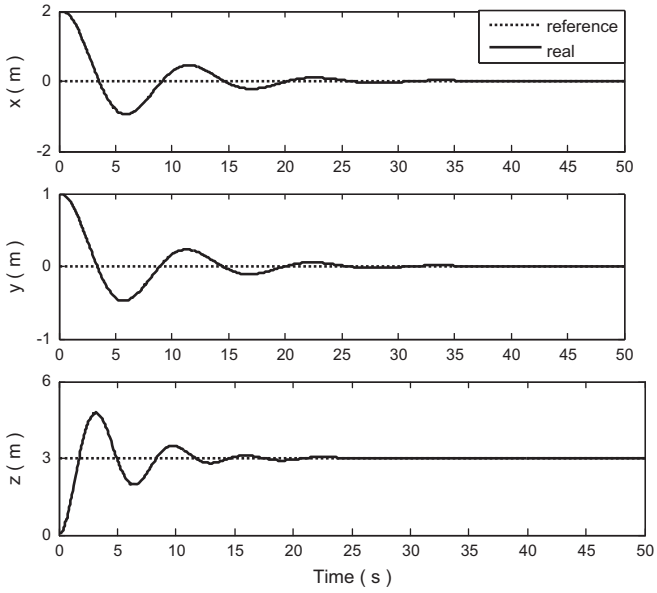

Fig. 2. The positions (x,y,z), PID control and SMC.

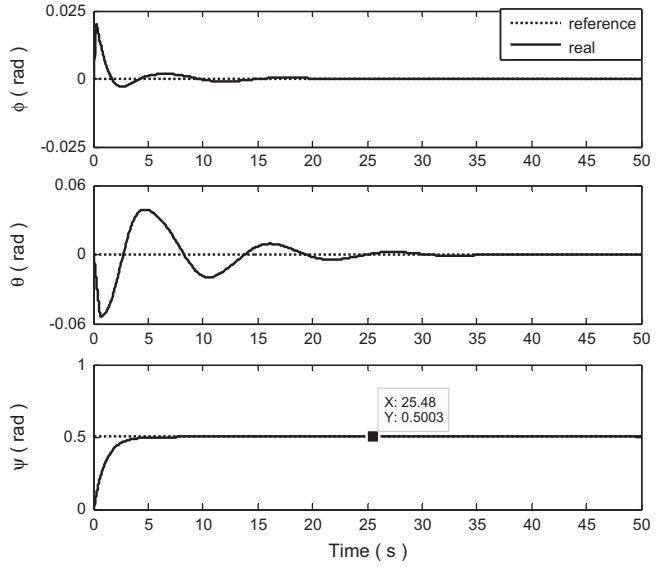

Fig. 3. The angles (ϕ,θ,ψ), PID control and SMC.

Proof 2. The stability of the subsystem is illustrated by Lyapunov theory as follows.

Consider the Lyapunov function candidate:

$$V = \frac{1}{2}s^T s$$

Invoking Eqs. (13) and (14), the time derivative of V is

$$\begin{aligned}\dot{V} &= s^T\dot{s} = s^T[c_1\dot{e}_1 + c_2\dot{e}_2 + c_3\dot{e}_3 + \dot{e}_4] \\ &= s^T\left(-M\mathrm{sgn}(s) + c_2 d_2 + c_3\frac{\partial f_2}{\partial y_2}d_2 + \frac{\partial f_2}{\partial y_3}d_3\right) \\ &< -\lambda s^T s - (M - (c_2\bar{d}_2 + c_3\beta_2\bar{d}_2)||E_1||_2 - \beta_3\bar{d}_4||\xi(x)||_2)||s||_1 \\ &= -\lambda s^T s - \rho||s||_1 \le 0.\end{aligned}$$

Therefore, under the controllers, the subsystem state trajectories can reach, and, thereafter, stay on the manifold $S=0$ in finite-time.

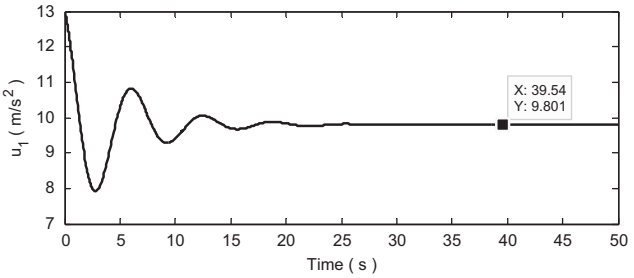

Fig. 4. The controller u_1, PID control and SMC.

Table 1
Quadrotor model parameters.

Variable	Value	Units
m	2.0	kg
$I_x = I_y$	1.25	Ns^2/rad
I_z	2.2	Ns^2/rad
$K_1 = K_2 = K_3$	0.01	Ns/m
$K_4 = K_5 = K_6$	0.012	Ns/m
l	0.20	m
J_r	1	Ns^2/rad
b	2	Ns^2
d	5	N ms^2
g	9.8	m/s^2

Table 2
Controller parameters.

Variable	Value	Variable	Value
ω_1	1	ω_2	3
ξ_1	1	ξ_2	1
m'_1	5	m'_2	5
n'_1	7	n'_2	7
m_1	1	m_2	1
n_1	3	n_2	3
ε_1	10	ε_2	10
η_1	$L_1/\lvert s_2^{m_1/n_1}\rvert + \delta_1$	η_2	$L_2/\lvert s_4^{m_2/n_2}\rvert + \delta_2$
δ_1	0.1	δ_2	0.1
c_1	20	c_2	22
c_3	8	ρ	1
λ	0.1	β_1	0
β_2	0	β_3	2

4. Simulation results and analysis

In this section, the dynamical model of the quadrotor UAV in Eq. (2) is used to test the validity and efficiency of the proposed synthesis control scheme when faced with external disturbances. The simulations of typical position and attitude tracking are performed on Matlab 7.1.0.246/Simulink, which is equipped with a computer comprising of a DUO E7200 2.53 GHz CPU with 2 GB of RAM and a 100 GB solid state disk drive. Moreover, the performance of the synthesis control is demonstrated through the comparison with the control method in [29], which used a rate bounded PID controller and a sliding mode controller for the fully actuated subsystem, and, a SMC approach for the underactuated subsystem.

4.1. PID control and SMC

In this section, more details of the PID control and SMC method for a quadrotor UAV has been introduced, meanwhile, the simulation results and analysis, which verify the effectiveness of the synthesis control scheme, can be found in [29]. The approximate

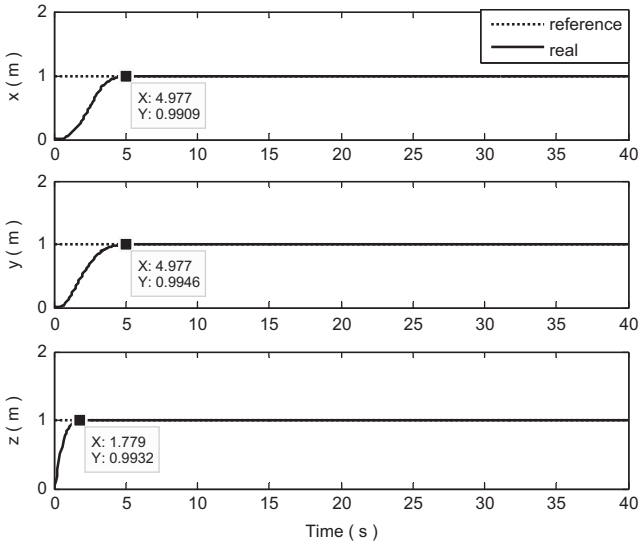

Fig. 5. The positions (x,y,z), novel robust TSMC and SMC.

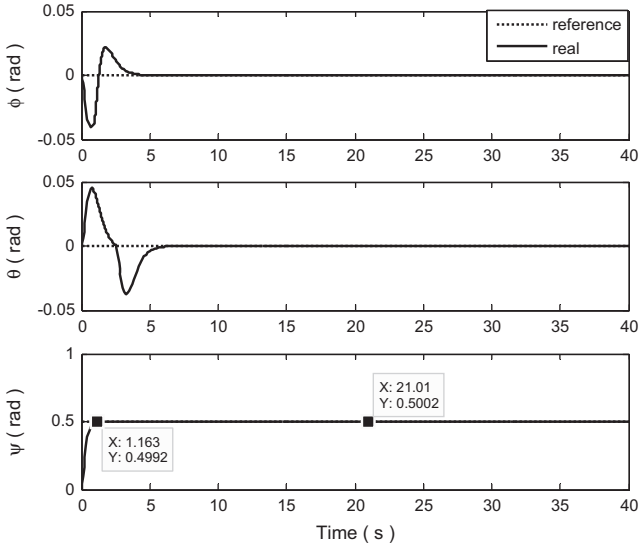

Fig. 6. The angles (ϕ,θ,ψ), novel robust TSMC and SMC.

simulation tests are shown in Figs. 2–4, however, the research objects are slightly changed to make obvious comparisons with the following simulation tests.

4.2. Novel robust TSMC and SMC

In this section, in order to justify the effectiveness of the proposed synthesis control method, the position and attitude tracking of the quadrotor have been performed.

The initial position and angle values of the quadrotor for the simulation tests are [0, 0, 0]m and [0, 0, 0]rad. In addition, the quadrotor's model variables are listed in Table 1.

The desired/reference position and angle values are used in simulation tests: $x_d=1$ m, $y_d=1$ m, $Z_d=1$ m, $\phi_d=\theta_d=0$ rad, $\psi_d=\pi/6.28$ rad. Besides, The controller parameters are listed in Table 2. The simulation results are shown in Figs. 5–10.

The overall control scheme managed to effectively hold the quadrotor's horizontal position and attitude in finite-time, as shown in Figs. 5 and 6. The finite-time convergence of the state variables z and ψ is clearly faster than the other state variables, therefore, it is safe to consider the pitch angle ψ as time invariant after 1.163 s. In addition, the altitude z reaches its reference value

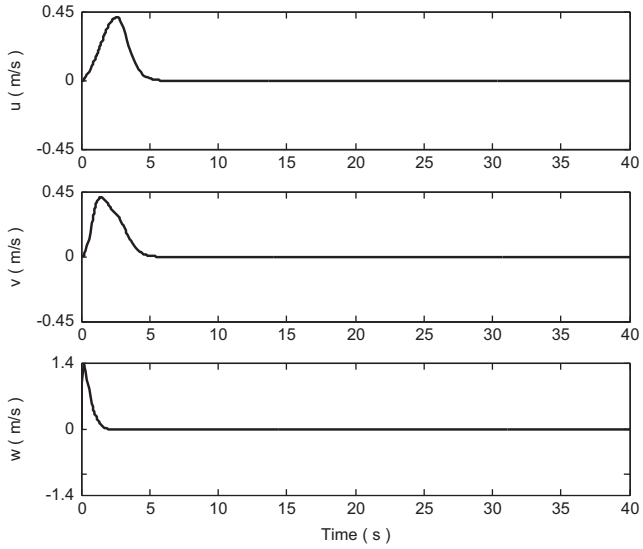

Fig. 7. The linear velocities (u,v,w), novel robust TSMC and SMC.

under the controller u_1 after 1.779 s, thus, it is reliable to consider the controller u_1 as time invariant after 1.779 s. These verify the matrix Q is time invariant in short finite-time. The other state variables reach their desired values after about 5 s. Even though the smooth curves of the state variables ϕ and θ show that they have certain oscillation amplitudes, the amplitudes are varying from -0.05 rad and 0.05 rad. According to the initial conditions, parameters and desired/reference values, the convergence time of the state variables z and ψ is essentially consistent with the values calculated by invoking Eqs. (7a) and (7b) and . This demonstrates the effectiveness of the proposed synthesis control scheme.

The linear and angular velocities, displayed in Figs. 7 and 8, respectively, exhibit the same behavior as the corresponding positions and angles. Indeed, these state variables are driven to their steady states as expected. This, once again, demonstrates the effectiveness of the synthesis control scheme.

The behavior of the sliding variables (s_2,s_4 and s), shown in Fig. 9, follows the expectations as all the variables converge to their sliding surfaces. Furthermore, as desired, the finite-time convergence of s_2 and s_4 is obviously faster than the finite-time convergence of s. Similarly, this exhibits the same behavior as shown in Figs. 5 and 6.

Seen from Fig. 10, it can be found that the four control input variables converge to their steady state values (19.66,0,0,0) after several seconds, respectively. Besides, $u_1 \neq 0$, this also verifies the matrix Q is time invariant in short finite-time. In spite of the high initial values, u_1 and u_4 are almost no oscillation amplitudes. This also denotes that the time derivative of u_1 trends to zero. Thus, compared with the equations in [29], Eq. (11) is greatly simplified.

Finally, the robustness of the proposed overall control method is demonstrated by considering the aerodynamic forces and moments and air drag taken as the external disturbances into the dynamical model of the quadrotor. Furthermore, these disturbance terms are also applied to the controller design. As a result, the effects of these disturbance terms are invisible on all the state variables, sliding variables, and controllers.

5. Discussion

The extensive simulation tests have been performed to evaluate the different synthesis control schemes which are based on position and attitude tracking of the quadrotor UAV. It can be

Please cite this article as: Xiong J-J, Zheng E-H. Position and attitude tracking control for a quadrotor UAV. ISA Transactions (2014), http://dx.doi.org/10.1016/j.isatra.2014.01.004

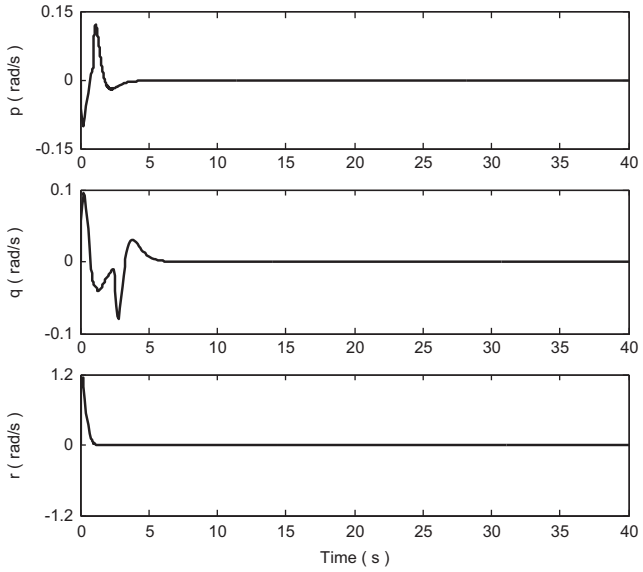

Fig. 8. The angular velocities (p,q,r), novel robust TSMC and SMC.

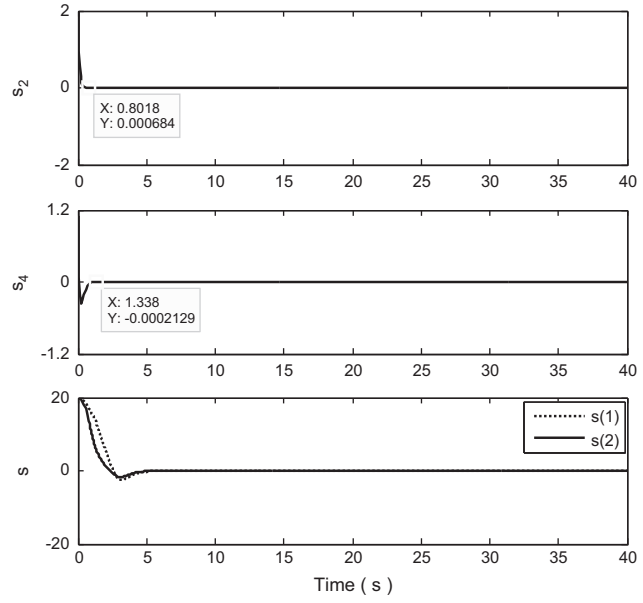

Fig. 9. The sliding variables (s_2,s_4,s), novel robust TSMC and SMC.

clearly seen that while all the state variables converge to their reference values as desired in finite-time, the convergence time is obviously different. It was shown that the synthesis control method based on the novel robust TSMC and SMC is a more reliable and effective approach to perform the tracking control for the quadrotor UAV.

6. Conclusion

This work studies the position and attitude tracking control of a small quadrotor UAV using the proposed control method based on the aforementioned control algorithms. In order to further test the performances of the designed controllers, the dynamical model of the quadrotor along with the controllers is simulated on Matlab/Simulink. The main conclusions are summarized as follows. (a) The six degrees of freedom converge to their desired/reference values in finite-time, respectively. (b) The convergence time of the state

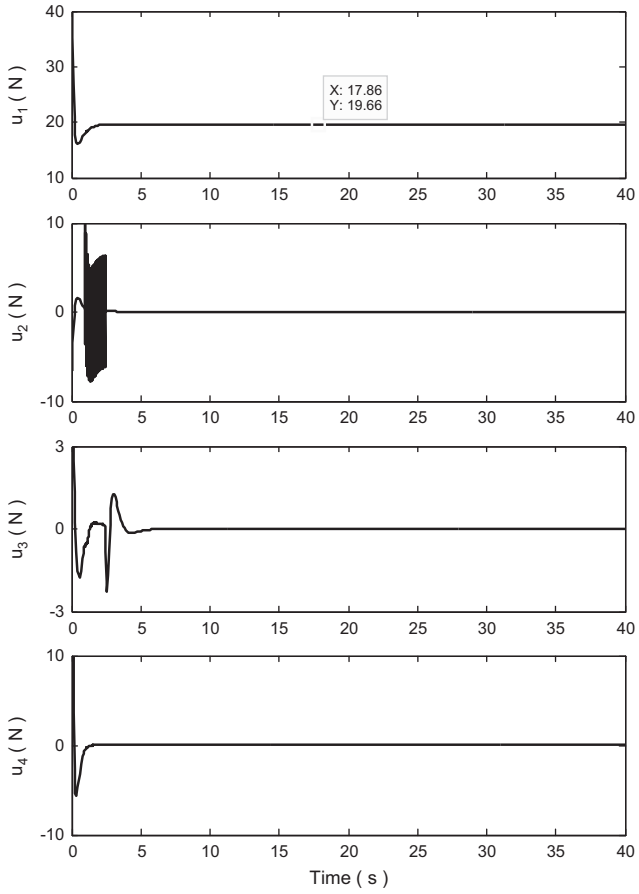

Fig. 10. The controllers (u_1,u_2,u_3,u_4), novel robust TSMC and SMC.

variables z and ψ is essentially consistent with the theoretically calculated values. (c) Compared to other variables, the pitch angle ψ and the controller u_1 become time invariants in short time. (d) The four control input variables converge to their steady values in finite-time,u_1 and u_4 are almost no oscillation amplitudes. All above, the effectiveness and robustness of the proposed synthesis control method have been demonstrated, and, the presented simulation results are promising at the position and attitude tracking control for the aircraft.

Acknowledgment

This work was partially supported by the National Natural Science Foundation of China (60905034).

References

[1] Raffo GV, Ortega MG, Rubio FR. An integral predictive/nonlinear $H\infty$ control structure for a quadrotor helicopter. Automatica 2010;46:29–39.
[2] Derafa L, Benallegue A, Fridman L. Super twisting control algorithm for the attitude tracking of a four rotors UAV. J Frankl Inst 2012;349:685–99.
[3] Luque-Vega L, Castillo-Toledo B, Loukianov AG. Robust block second order sliding mode control for a quadrotor. J Frankl Inst 2012;349:719–39.
[4] Garcia-Delgado L, Dzul A, Santibáñez V, Llama M. Quadrotors formation bansed on potential functions with obstacle avoidance. IET Control Theory Appl 2012;6(12):1787–802.
[5] Alexis K, Nikolakopoulos G, Tzes A. Model predictive quadrotor control: attitude, altitude and position experimental studies. IET Control Theory Appl 2012;6(12):1812–27.
[6] Nekoukar V, Erfanian A. Adaptive fuzzy terminal sliding mode control for a class of MIMO uncertain nonlinear systems. Fuzzy Sets Syst 2011;179:34–9.
[7] Ashrafiuon H, Scott-Erwin R. Sliding mode control of under-actuated multi-body systems and its application to shape change control. Int J Control 2008;81(12):1849–58.

[8] Jin Y, Chang PH, Jin ML, Gweon DG. Stability guaranteed time-delay control of manipulators using nonlinear damping and terminal sliding mode. IEEE Trans Ind Electron 2013;60(8):3304–17.
[9] Zhi-hong M, Paplinski AP, Wu HR. A robust MIMO terminal sliding mode control scheme for rigid robotic manipulators. IEEE Trans Autom Control 1994;39(12):2464–9.
[10] Wang L, Chai T, Zhai L. Neural-network-based terminal sliding-mode control of robotic manipulators including actuator dynamics. IEEE Trans Ind Electron 2009;56(9):3296–304.
[11] Tan CP, Yu X, Man Z. Terminal sliding mode observers for a class of nonlinear systems. Automatica 2010;46(8):1401–4.
[12] Wu Y, Yu X, Man Z. Terminal sliding mode control design for uncertain dynamic systems. Syst Control Lett 1998;34:281–7.
[13] Man Z, O'Day M, Yu X. A robust adaptive terminal sliding mode control for rigid robotic manipulators. J Intell Robotic Syst 1999;24:23–41.
[14] Feng Y, Yu X, Man Z. Non-singular terminal sliding mode control of rigid manipulators. Automatica 2002;38:2159–67.
[15] Hong Y, Xu Y, Huang J. Finite-time control for robot manipulators. Syst Control Lett 2002;46:243–53.
[16] Yu S, Yu X, Shirinzadeh B, Man Z. Continuous finite-time control for robotic manipulators with terminal sliding mode. Automatica 2005;41:1957–64.
[17] Chen SY, Lin FJ. Robust nonsingular terminal sliding-mode control for nonlinear magnetic bearing system. IEEE Trans Control Syst Technol 2011;19(3):636–43.
[18] Chen M, Wu QX, Cui RX. Terminal sliding mode tracking control for a class of SISO uncertain nonlinear systems. ISA Trans 2013;52:198–206.
[19] Xu R, Özgüner Ü. Sliding mode control of a quadrotor helicopter. In: Proceedings of the 45th IEEE conference on decision and control, San Diego, USA. vol. 12: 2006. p. 4957–62.
[20] Mokhtari A, Benallegue A, Orlov Y. Exact linearization and sliding mode observer for a quadrotor unmanned aerial vehicle. Int J Robot Autom 2006;21:39–49.
[21] Benallegue A, Mokhtari A, Fridman L. High-order sliding-mode observer for a quadrotor UAV. Int J Robust Nonlinear Control 2008;18:427–40.
[22] Sharifi F, Mirzaei M, Gordon BW Zhang YM. Fault tolerant control of a quadrotor UAV using sliding mode control. In: Proceedings of the conference on control and fault tolerant systems. Nice, France; 2010. p. 239–44.
[23] Besnard L, Shtessel YB, Landrum B. Quadrotor vehicle control via sliding mode controller driven by sliding mode disturbance observer. J Frankl Inst 2012;349:658–84.
[24] Efe MO. Neural network assisted computationally simple $PI^{\lambda}D^{\mu}$ control of a quadrotor UAV. IEEE Trans Ind Informa 2011;7(2):354–61.
[25] Lim H, Park J, Lee D, Kim HJ. Build your own quadrotor: open-source projects on unmanned aerial vehicles. IEEE Robot Autom Mag 2012;19(3):33–45.
[26] Zuo Z. Trajectory tracking control design with command-filtered compensation for a quadrotor. IET Control Theory Appl 2010;4(11):2343–55.
[27] Das A, Lewis F, Subbarao K. Backstepping approach for controlling a quadrotor using Lagrange from dynamics. J Intell Robot Syst 2009;56:127–51.
[28] Alexis K, Nikolakopoulos G, Tzes A. Switching model predictive attitude control for a quadrotor helicopter subject to atmospheric disturbances. Control Eng Pract 2011;19(10):1195–207.
[29] Xu R, Özgüner Ü. Sliding mode control of a class of underactuated systems. Automatica 2008;44:233–41.
[30] Yu X, Man Z. Fast terminal sliding-mode control design for nonlinear dynamical systems. IEEE Trans Circ Syst—Fundam Theory Appl 2002;49(2):261–4.

Please cite this article as: Xiong J-J, Zheng E-H. Position and attitude tracking control for a quadrotor UAV. ISA Transactions (2014), http://dx.doi.org/10.1016/j.isatra.2014.01.004